$\phi(2170)$ state as a vector strangeonium hybrid meson

Wei Chen

Sun Yat-Sen University

Baryons 2025, ICC Jeju, Korea, Nov. 10-14, 2025

Based on: arXiv:2506.22412

Collaborators: Shuang-Hong Li, Zhuo-Ran Huang, Hong-Ying Jin

Outline

Quark model and Exotic hadrons

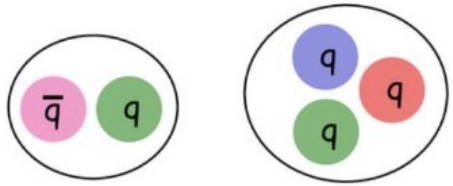

- **Quark Model:** $q\bar{q}$ mesons and qqq baryons
- **Exotic Hadrons:** hadrons beyond QM, such as multiquarks, hybrids, glueballs...
- **Hybrids and Glueballs:** very distinctive predictions of QCD!

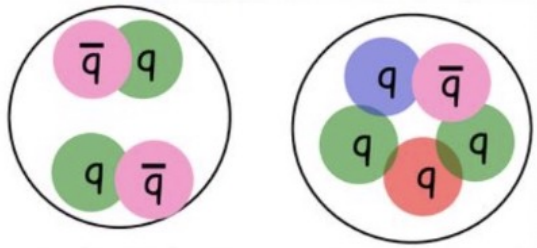

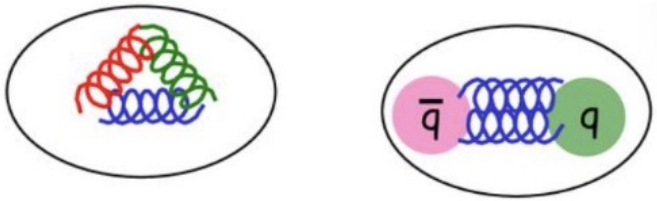

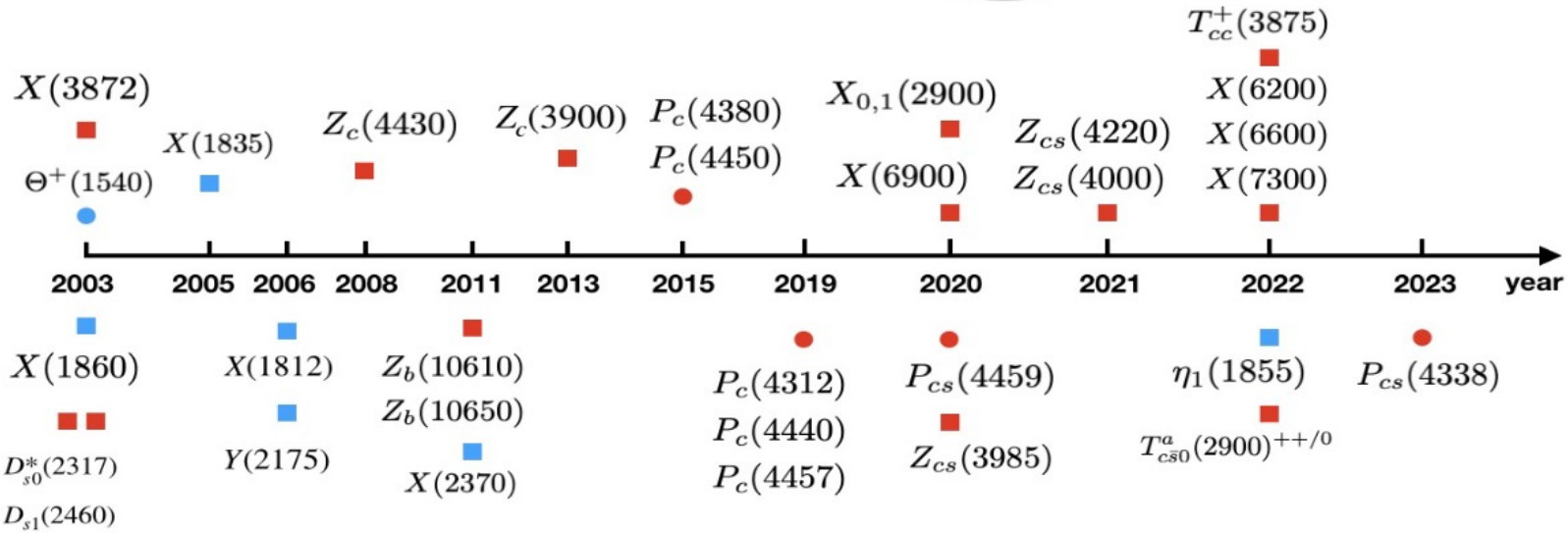

Hybrid meson: $[q\bar{q}]_{\mathbf{8_c}}$ + one excited gluonic field

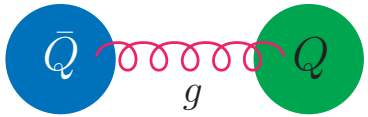

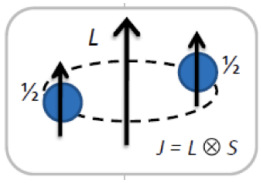

$$\mathbf{8} \otimes \mathbf{8} = \mathbf{1} \oplus \mathbf{8} \oplus \mathbf{8} \oplus \mathbf{10} \oplus \mathbf{10}^* \oplus \mathbf{27}$$

Model	$J^{PC}_{q\bar{q}'}$	J^{PC}_{g}	J^{PC}	Mass (GeV/c^2)
Bag [2, 3]	0^{-+}	1^{+-} (TE)	1^{--}	~ 1.7
	1^{--}	1^{+-} (TE)	$(0,\mathbf{1},2)^{-+}$	$\sim 1.3, 1.5, 1.9$
	0^{-+}	1^{--} (TM)	1^{+-}	heavier
	1^{--}	1^{--} (TM)	$(0,1,2)^{++}$	heavier
Flux tube [4, 5]	0^{-+}	1^{+-}	1^{--}	1.7-1.9
	1^{--}	1^{+-}	$(0,\mathbf{1},2)^{-+}$	1.7-1.9
	0^{-+}	1^{-+}	1^{++}	1.7-1.9
	1^{--}	1^{-+}	$(\mathbf{0},1,\mathbf{2})^{+-}$	1.7-1.9
Constituent gluon [6]/[7]	0^{-+}	1^{--}	1^{+-}	1.3-1.8 / 2.1
	1^{--}	1^{--}	$(0,1,2)^{++}$	1.3-1.8 / 2.2
	1^{+-}	1^{--}	$(0,\mathbf{1},2)^{-+}$	1.8-2.2 / 2.2
	$(0,1,2)^{++}$	1^{--}	$1^{--}, (\mathbf{0},1,2)^{--}, (1,2,3)^{--}$	1.8-2.2 / 2.3
Constituent gluon / LQCD [8, 9]	0^{-+}	1^{+-}	1^{--}	(2.3)
	1^{--}	1^{+-}	$(0,\mathbf{1},2)^{-+}$	(2.1, 2.0, 2.4)
	1^{+-}	1^{+-}	$(0,1,2)^{++}$	(> 2.4)
	$(0,1,2)^{++}$	1^{+-}	$1^{+-}, (\mathbf{0},1,\mathbf{2})^{+-}, (1,\mathbf{2},3)^{+-}$	(> 2.4)

arXiv:1208.5125

Hybrid candidates: $\pi_1(1400), \pi_1(1600), \pi_1(2015)$

They quantum numbers are identified as $I^G J^{PC} = 1^- 1^{-+}$:

- $\pi_1(1400)$: observed in the $\eta\pi$ and $\rho\pi$ channels;
- $\pi_1(1600)$: observed in the $\rho\pi$, $\eta'\pi$, $f_1\pi$ and $b_1\pi$ channels;
- $\pi_1(2015)$: observed in the $f_1\pi$ and $b_1\pi$ channels;
- $\pi_1(1400)$ and $\pi_1(1600)$ may be the same state! (PRL,122(2019)042002)

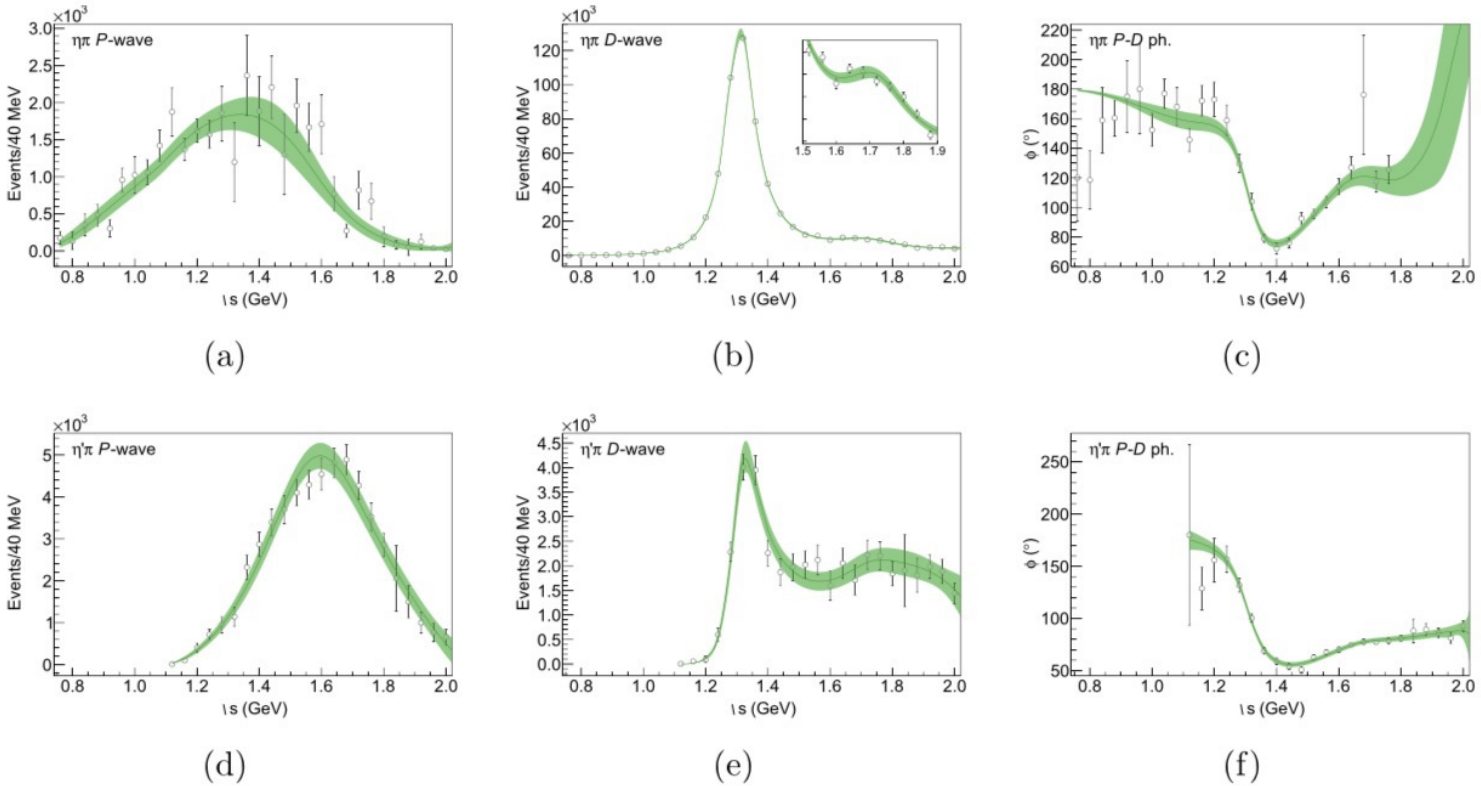

Observation of $\eta_1(1855)$

In 2022, BESIII found an isoscalar structure $\eta_1(1855)$ with $I^G J^{PC} = 0^+1^{-+}$ in the process $J/\psi \to \gamma\eta_1(1855) \to \gamma\eta\eta'$ (PRL129 (2022) 192002; PRD106 (2022) 072012):

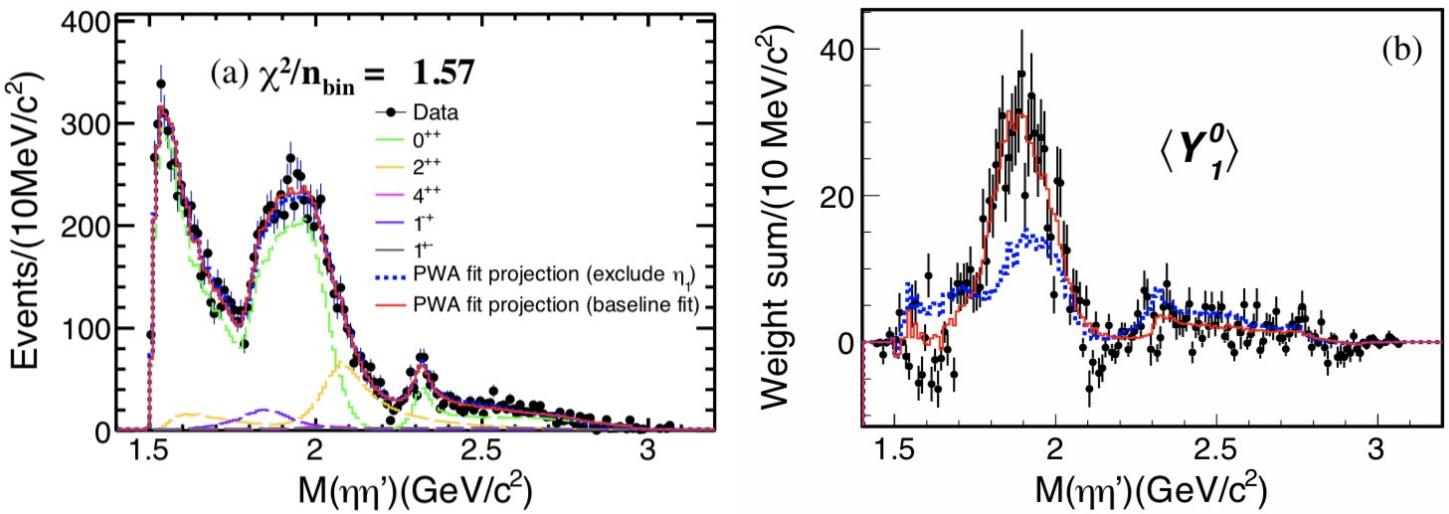

$$\eta_1(1855): M = 1855 \pm 9^{+6}_{-1}\ \mathrm{MeV}/c^2,$$
$$\Gamma = 188 \pm 18^{+3}_{-8}\ \mathrm{MeV}.$$

Theoretical calculations of the 1^{-+} hybrids

Prog.Part. Nucl. Phys. (2015) 82 21–58

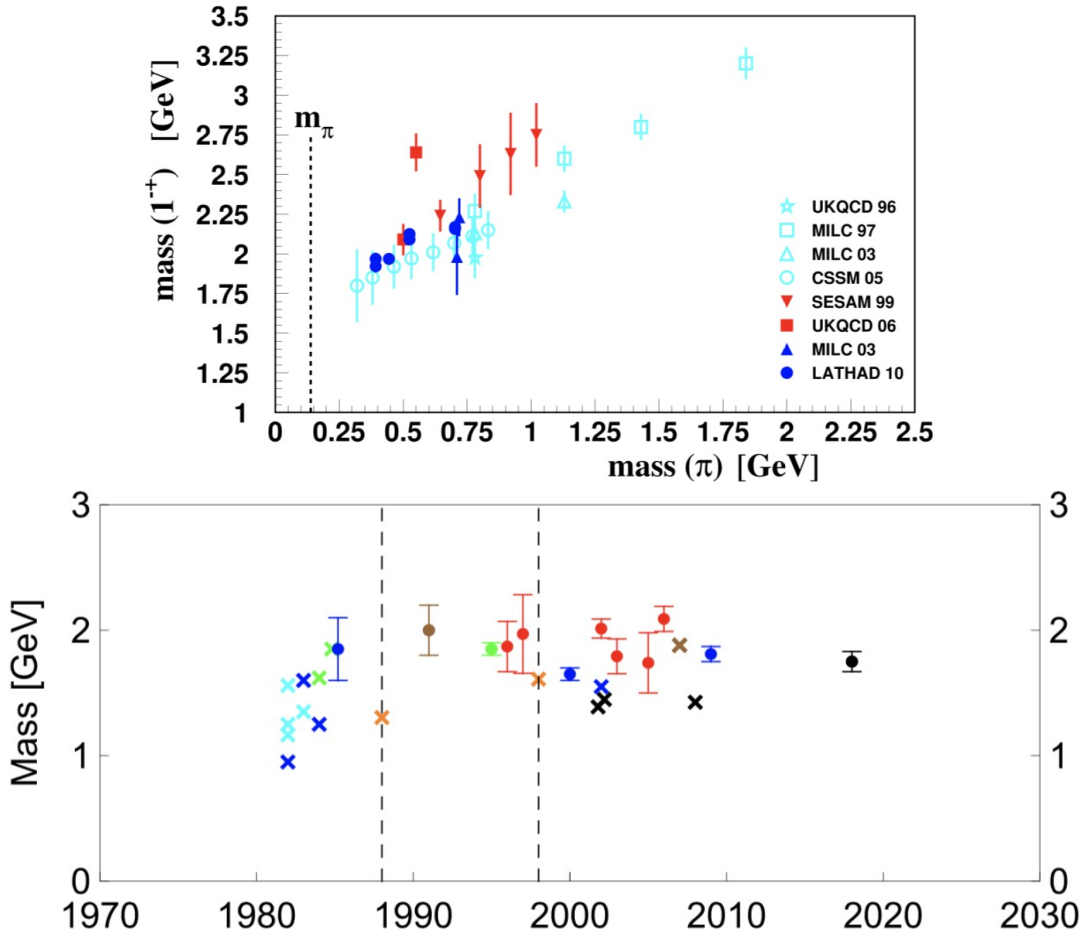

Theoretical predictions of the 1^{-+} hybrids are consistent with the masses for $\pi_1(1600)$ and $\eta_1(1855)$.

$\phi(2170)$

Observed by BaBar in 2006 in the ISR process $e^+e^- \to \phi f_0(980)\gamma$:

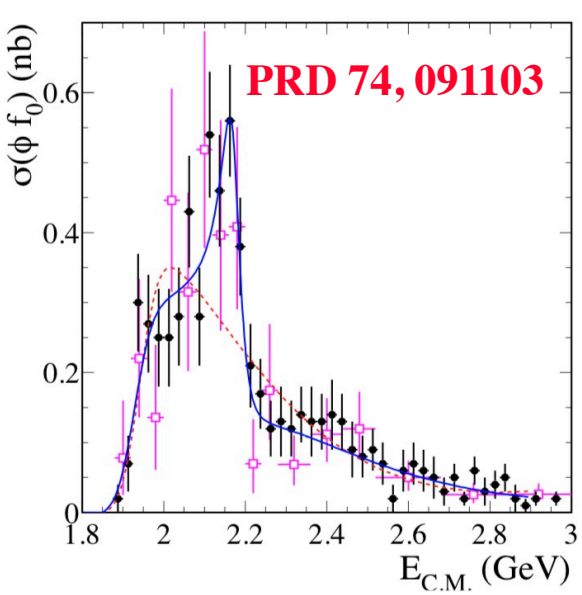

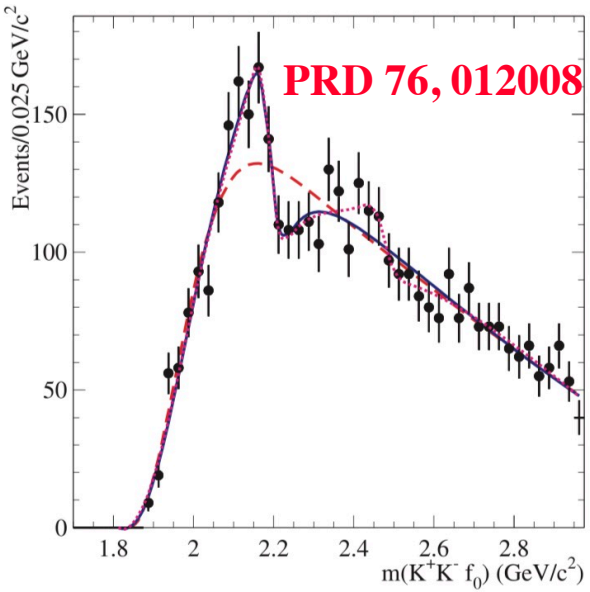

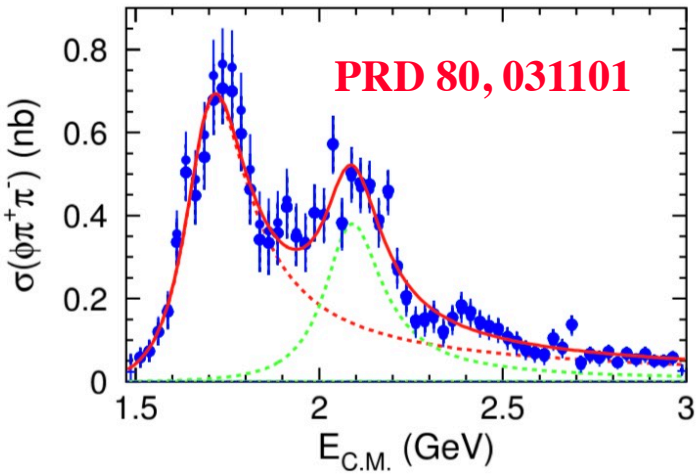

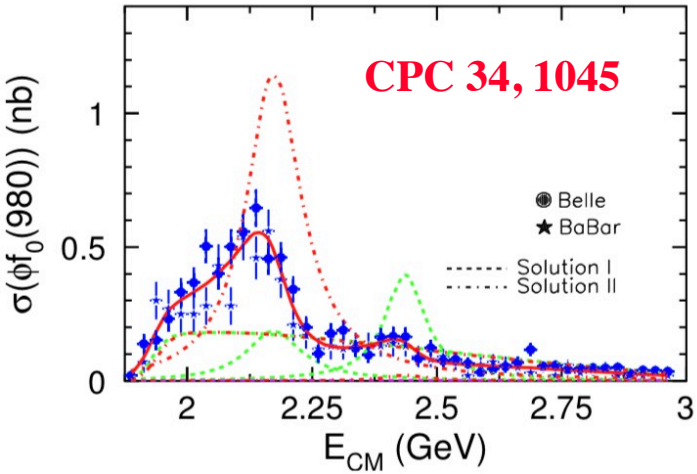

Theoretical interpretations of $\phi(2170)$

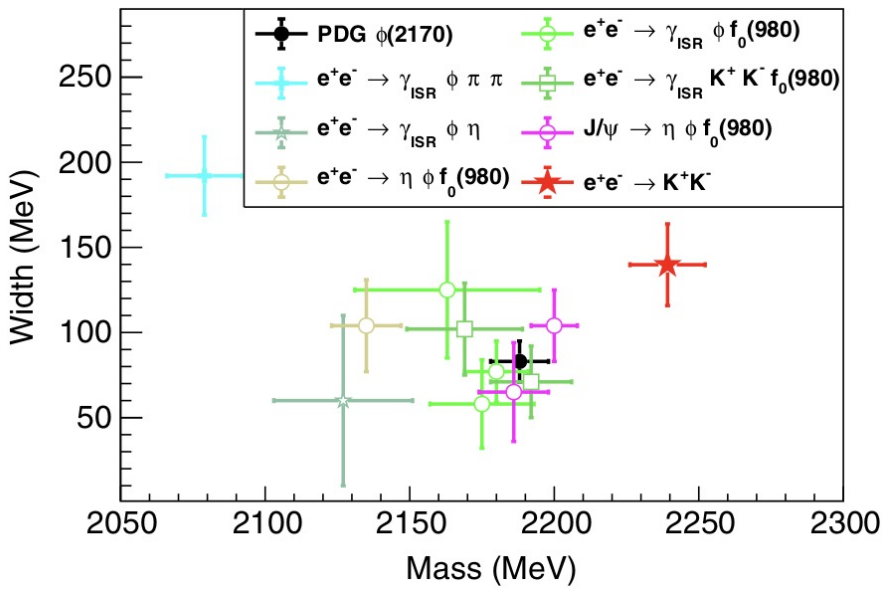

The present data can not determine the nature of $\phi(2170)$:

- $2\,^3D_1$ or $3\,^3S_1$ $s\bar{s}$ state: PRD85,074024; PRD99,074015;PLB657,49.
- Tetraquark $ss\bar{s}\bar{s}$ state: NPA791,106; PRD98, 014011;D78,034012;D99,036014.
- Molecular $\Lambda\bar{\Lambda}$ state: PRD96,074027; PRD87,054034.
- $\phi f_0(980)$ resonance with FSI: PRD80,054011.
- Three body ϕKK system: PRD78, 074031; PRD83, 116002.
- **Hybrid meson $\bar{s}gs$:** PLB650,390;PRD59, 034016;PRD100(2019),034012.

QCD Sum Rules

- Study two-point correlation function of current $J_\mu(x)$ with the same quantum numbers with hadron state:

$$\Pi_{\mu\nu}(q^2) = i \int d^4x e^{iq\cdot x} \langle \Omega | T[J_\mu(x) J_\nu^\dagger(0)] | \Omega \rangle$$

- Classify states $|X\rangle$ by coupling to current $\langle \Omega | J_\mu(x) | X \rangle \neq 0$
- Hadron level: described by the dispersion relation

$$\begin{aligned} \Pi(q^2) &= \frac{(q^2)^N}{\pi} \int \frac{\mathrm{Im}\Pi(s)}{s^N(s - q^2 - i\epsilon)} ds + \sum_{n=0}^{N-1} b_n (q^2)^n, \\ \rho(s) &= \frac{1}{\pi} \mathrm{Im}\Pi(s) = \sum_n \delta(s - m_n^2) \langle 0|J|n\rangle \langle n|J^\dagger|0\rangle \end{aligned}$$

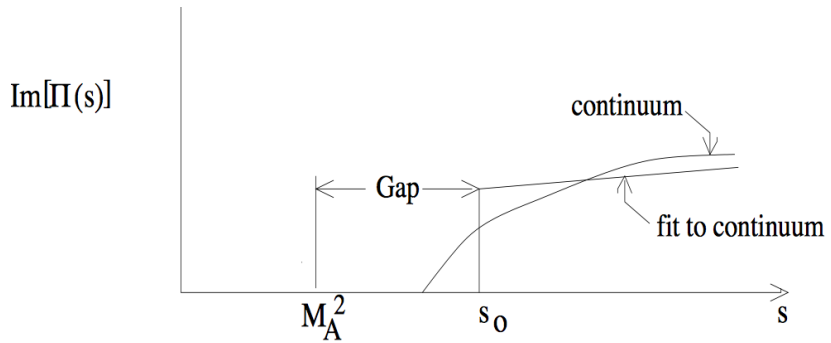

Hybrid Sum Rules

The hybrid interpolating currents:

$$
\begin{aligned}
J_\mu &= g_s\bar{s}\frac{\lambda^a}{2}\gamma^\nu G^a_{\mu\nu}s, && J^{PC}=1^{-+},0^{++},\\
J_\mu &= g_s\bar{s}\frac{\lambda^a}{2}\gamma^\nu\gamma_5 G^a_{\mu\nu}s, && J^{PC}=1^{+-},0^{--},\\
J_{\mu\nu} &= g_s\bar{s}\frac{\lambda^a}{2}\sigma^\alpha_\mu\gamma_5 G^a_{\alpha\nu}s, && J^{PC}=2^{-+},1^{++},1^{-+},0^{-+},\\
\tilde{J}_\mu &= g_s\bar{s}\frac{\lambda^a}{2}\gamma^\nu \tilde{G}^a_{\mu\nu}s, && J^{PC}=1^{++},0^{-+},\\
\tilde{J}_\mu &= g_s\bar{s}\frac{\lambda^a}{2}\gamma^\nu\gamma_5 \tilde{G}^a_{\mu\nu}s, && J^{PC}=1^{--},0^{+-},\\
\tilde{J}_{\mu\nu} &= g_s\bar{s}\frac{\lambda^a}{2}\sigma^\alpha_\mu\gamma_5 \tilde{G}^a_{\alpha\nu}s, && J^{PC}=2^{++},1^{-+},1^{++},0^{++},\\
J_{\mu\nu\sigma} &= g_s\bar{q}\gamma_\mu\gamma_5 G_{\nu\sigma}q, && J^{PC}=2^{+-},2^{--},1^{+-},1^{--},0^{+-},0^{--}.
\end{aligned}
$$

Laplace Sum Rules Analyses (LSRs)

- Borel transform: suppress the contributions of continuum and higher excited states in correlation functions:

$$\Pi_k(M_B^2) = M_B^2 \lim_{\substack{N,Q^2\to\infty \\ M_B^2=Q^2/N}} \frac{\left(-Q^2\right)^N}{\Gamma(N)}\left(\frac{d}{dQ^2}\right)^N\left\{(-Q^2)^k\Pi(Q^2)\right\},$$

- Quark-hadron duality: Laplace Sum Rules with QCD spectral function

$$\mathcal{L}_k\left(s_0, M_B^2\right) = \int_{4m_s^2}^{s_0} ds e^{-s/M_B^2}\rho(s)s^k = f_X^2 m_X^{2k} e^{-m_X^2/M_B^2}\,.$$

where s_0 is continuum threshold and M_B is the Borel parameter.

Feynman diagrams at LO of α_s

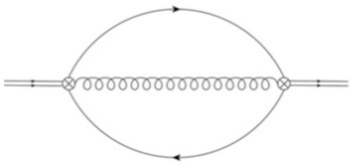

(a) Diagram I (LO perturbation theory)

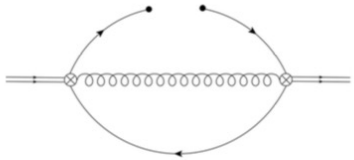

(b) Diagram II (dimension-three)

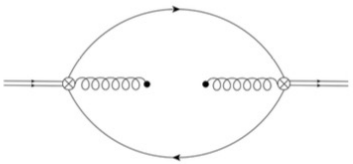

(c) Diagram III (dimension-four)

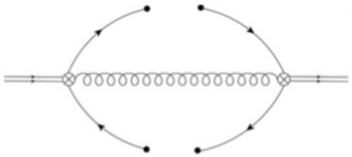

(d) Diagram IV (dimension-six)

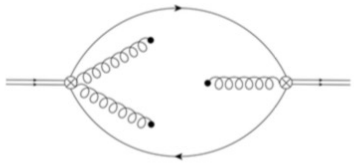

(e) Diagram V (dimension-six)

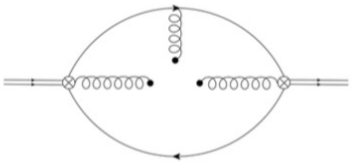

(f) Diagram VI (dimension-six)

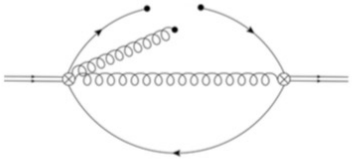

(g) Diagram VII (dimension-five)

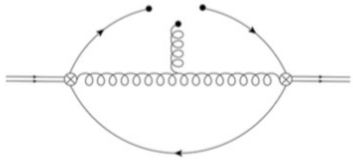

(h) Diagram VIII (dimension-five)

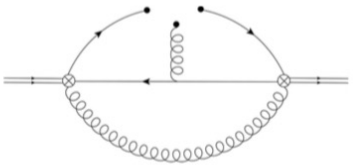

(i) Diagram IX (dimension-five)

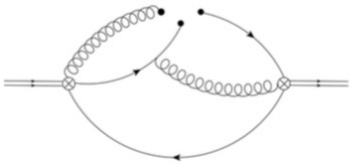

(j) Diagram X (dimension-five)

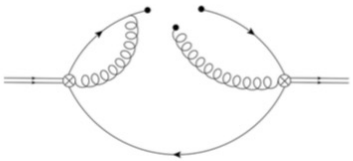

(k) Diagram XI (dimension-five)

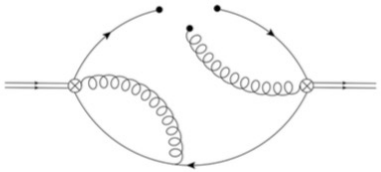

(l) Diagram XII (dimension-five)

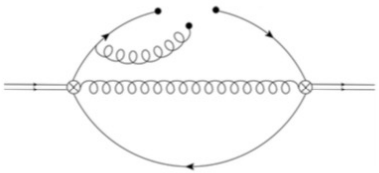

(m) Diagram XIII (dimension-five)

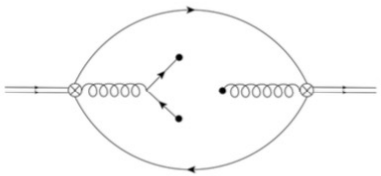

(n) Diagram XIV (dimension-five)

Correlation functions at LO

Two-point correlation functions at the leading order of α_s:

$$\begin{aligned}\Pi\left(q^2\right) =&\alpha_s\left(A_1 q^6+A_2 m^2 q^4\right)\log\left(\frac{-q^2}{\mu^2}\right)+\Big(A_4 q^2\langle\alpha G^2\rangle+\alpha_s(A_3 q^2 m\langle\bar{q}q\rangle+A_5\langle\bar{q}q\rangle^2\\&+A_6\langle g^3G^3\rangle+A_7 m\langle g\bar{q}\sigma Gq\rangle)\Big)\log\left(\frac{-q^2}{\mu^2}\right)+\alpha_s\Big(B_1 q^6+B_2 m^2 q^4\\&+B_3 q^2 m\langle\bar{q}q\rangle+B_4 q^2\langle\alpha G^2\rangle+B_5\langle\bar{q}q\rangle^2+B_6\langle g^3G^3\rangle+B_7 m\langle g\bar{q}\sigma Gq\rangle\Big)\end{aligned}$$

	0^{++}	1^{-+}	0^{--}	1^{+-}	0^{-+}	1^{++}	0^{+-}	1^{--}
A_1	$-\frac{1}{480\pi^3}$	$-\frac{1}{240\pi^3}$	$-\frac{1}{480\pi^3}$	$-\frac{1}{240\pi^3}$	$-\frac{1}{480\pi^3}$	$-\frac{1}{240\pi^3}$	$-\frac{1}{480\pi^3}$	$-\frac{1}{240\pi^3}$
A_2	0	$\frac{1}{12\pi^3}$	$\frac{1}{16\pi^3}$	$\frac{5}{48\pi^3}$	0	$\frac{1}{12\pi^3}$	$\frac{1}{16\pi^3}$	$\frac{5}{48\pi^3}$
A_3	$\frac{1}{3\pi}$	$-\frac{2}{9\pi}$	$-\frac{1}{3\pi}$	$-\frac{4}{9\pi}$	$\frac{1}{3\pi}$	$-\frac{2}{9\pi}$	$-\frac{1}{3\pi}$	$-\frac{4}{9\pi}$
A_4	$\frac{1}{24\pi}$	$-\frac{1}{36\pi}$	$\frac{1}{24\pi}$	$-\frac{1}{36\pi}$	$-\frac{1}{24\pi}$	$\frac{1}{36\pi}$	$-\frac{1}{24\pi}$	$\frac{1}{36\pi}$
A_5	0	0	0	0	0	0	0	0
A_6	0	0	0	0	0	0	0	0
A_7	$\frac{1}{9\pi}$	0	$\frac{11}{72\pi}$	$-\frac{19}{72\pi}$	$-\frac{1}{9\pi}$	0	$-\frac{11}{72\pi}$	$\frac{19}{72\pi}$

LSRs at LO

Mass prediction for the vector $\bar{s}Gs$ hybrid meson:

arXiv: 2506.22412

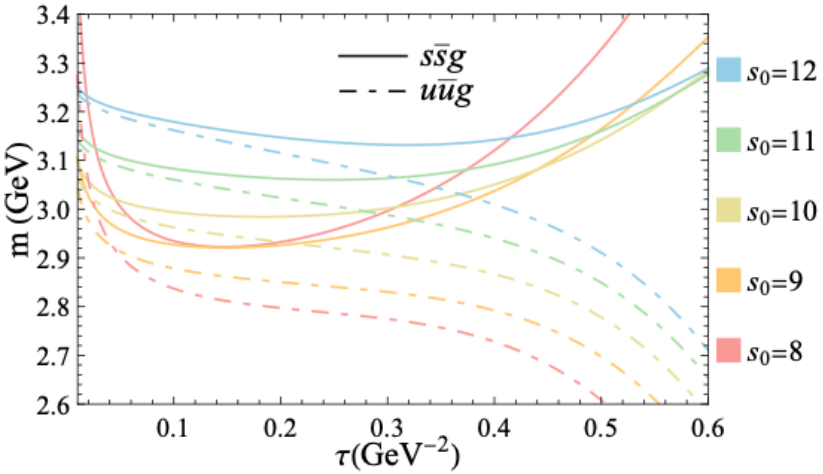

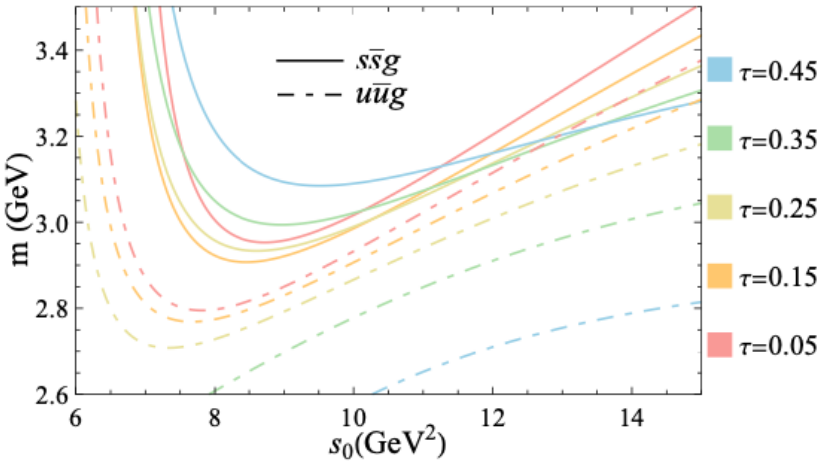

$m_X \sim 2.8 - 3.1$ GeV is much higher than the mass of $\phi(2170)$!

NLO Feynman diagrams

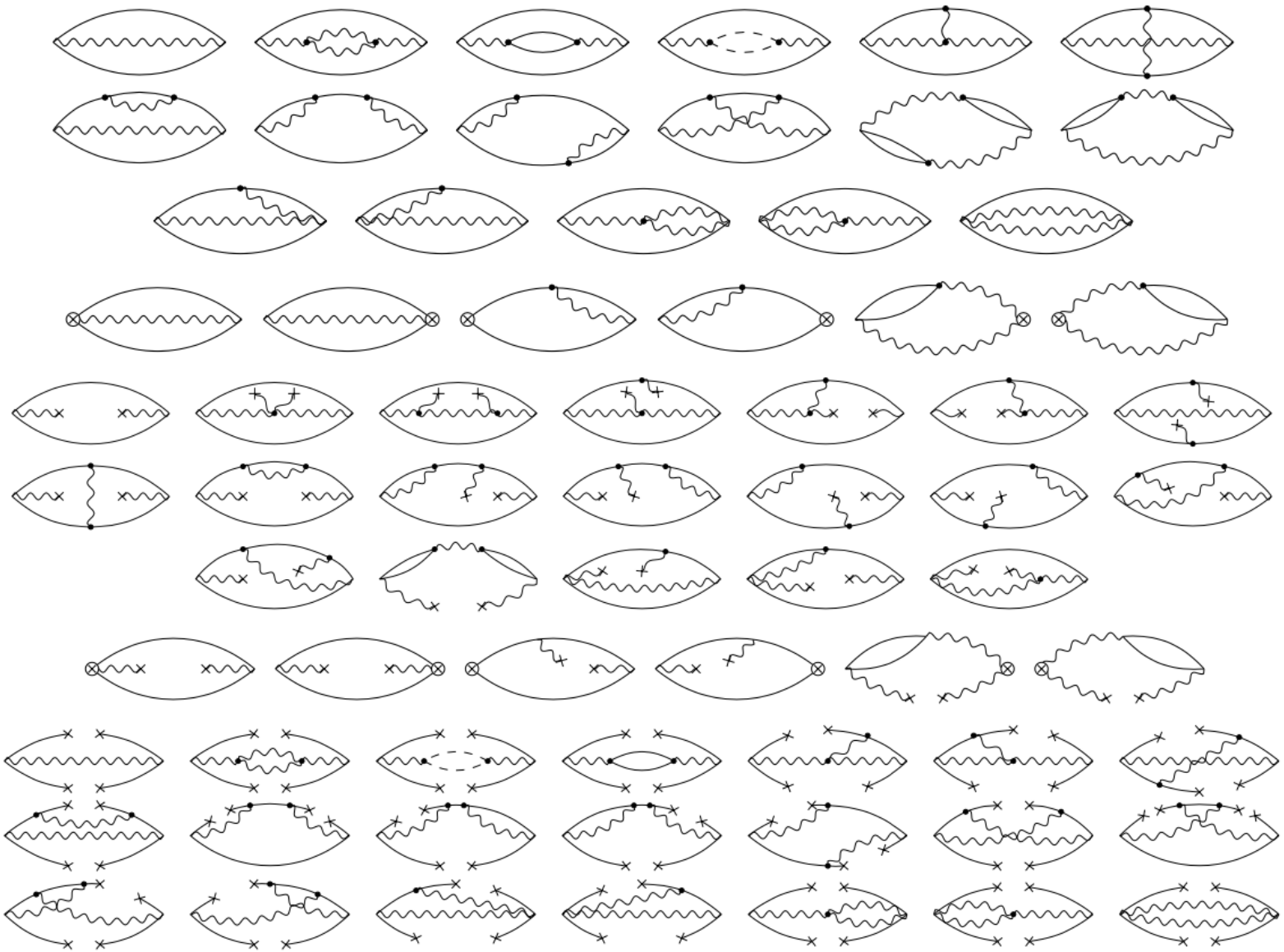

Correlation function at NLO

The renormalized 1^{--} hybrid current yields CF at NLO:

$$\begin{aligned}\Pi_v(q^2) =& -\log\left(-\frac{q^2}{\mu^2}\right)\left[\frac{(6n_f-35)\alpha_s^2q^6}{17280\pi^4}\log\left(-\frac{q^2}{\mu^2}\right)-\frac{(454n_f-6815)\alpha_s^2q^6}{172800\pi^4}+\frac{\alpha_sq^6}{240\pi^3}\right]\\&+\left[\frac{2\alpha_sq^2}{81\pi^2}\log\left(-\frac{q^2}{\mu^2}\right)-\frac{17\alpha_sq^2}{864\pi^2}+\frac{q^2}{36\pi}\right]\log\left(-\frac{q^2}{\mu^2}\right)\langle GG\rangle-\frac{4\alpha_s}{9\pi}q^2\log\left(-\frac{q^2}{\mu^2}\right)m\langle\overline{\Psi}\Psi\rangle\\&+\frac{1}{162}(24n_f+103)\alpha_s^2\log\left(-\frac{q^2}{\mu^2}\right)\langle\overline{\Psi}\Psi\rangle^2-\frac{4}{27}\alpha_s^2\log\left(-\frac{q^2}{\mu^2}\right)\left[\langle\bar{u}u\rangle^2+\langle\bar{d}d\rangle^2+\langle\bar{s}s\rangle^2\right]\\&+\frac{15}{32\pi}\alpha_s\log\left(-\frac{q^2}{\mu^2}\right)m\langle\overline{\Psi}G\Psi\rangle-\frac{77\pi\alpha_s}{54q^2}\langle\overline{\Psi}\Psi\rangle\langle\overline{\Psi}G\Psi\rangle.\end{aligned}$$

$$\begin{aligned}\Pi_s(q^2) =& -\log\left(-\frac{q^2}{\mu^2}\right)\left[\frac{(6n_f-35)\,\alpha_s^2q^6}{34560\pi^4}\log\left(-\frac{q^2}{\mu^2}\right)-\frac{(1722n_f-20945)\,\alpha_s^2q^6}{1036800\pi^4}+\frac{\alpha_sq^6}{480\pi^3}\right]\\&-\left[\frac{\alpha_sq^2}{27\pi^2}\log\left(-\frac{q^2}{\mu^2}\right)-\frac{115\alpha_sq^2}{1728\pi^2}+\frac{q^2}{24\pi}\right]\log\left(-\frac{q^2}{\mu^2}\right)\langle GG\rangle-\frac{\alpha_s}{3\pi}q^2\log\left(-\frac{q^2}{\mu^2}\right)m\langle\overline{\Psi}\Psi\rangle\\&+\frac{37}{162}\alpha_s^2\log\left(-\frac{q^2}{\mu^2}\right)\langle\overline{\Psi}\Psi\rangle^2+\frac{4}{27}\alpha_s^2\log\left(-\frac{q^2}{\mu^2}\right)\left[\langle\bar{u}u\rangle^2+\langle\bar{d}d\rangle^2+\langle\bar{s}s\rangle^2\right]\\&-\frac{15}{32\pi}\alpha_s\log\left(-\frac{q^2}{\mu^2}\right)m\langle\overline{\Psi}G\Psi\rangle+\frac{23\pi\alpha_s}{27q^2}\langle\overline{\Psi}\Psi\rangle\langle\overline{\Psi}G\Psi\rangle.\end{aligned}$$

NLO contributions

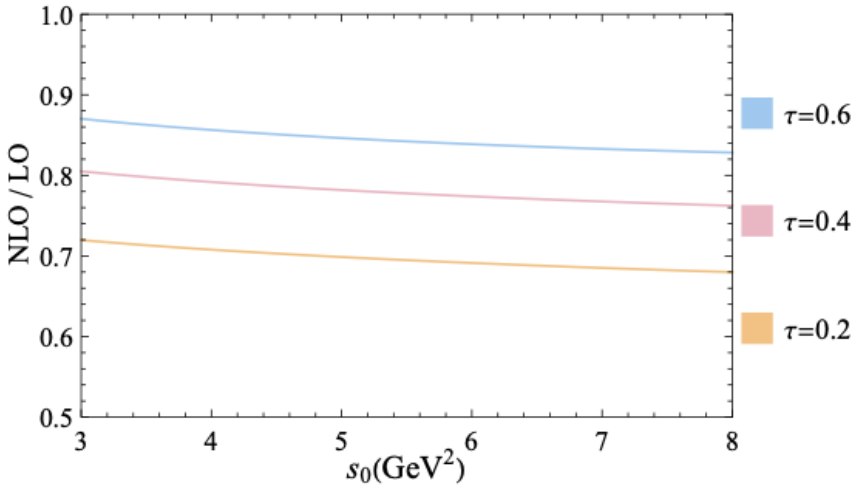

(a) Perturbative terms.

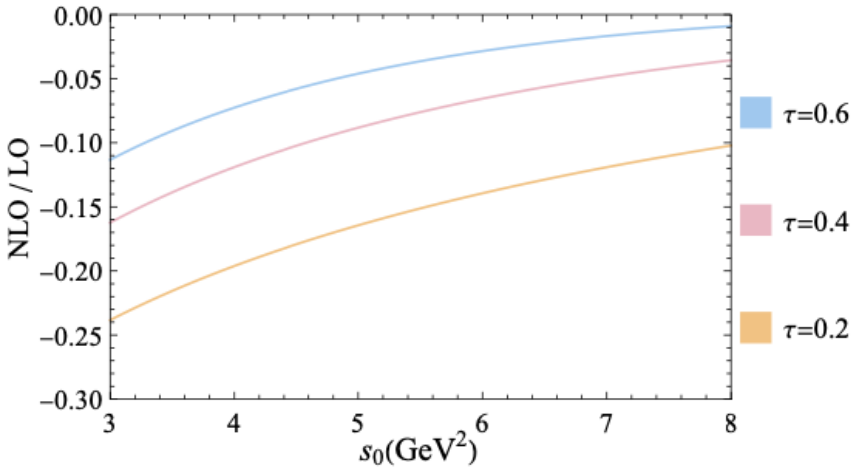

(b) $\langle GG \rangle$ terms.

The perturbative series converge very slow, where the NLO contributions are substantial!

NLO LSR analyses

Mass prediction for the vector $\bar{s}Gs$ hybrid meson:

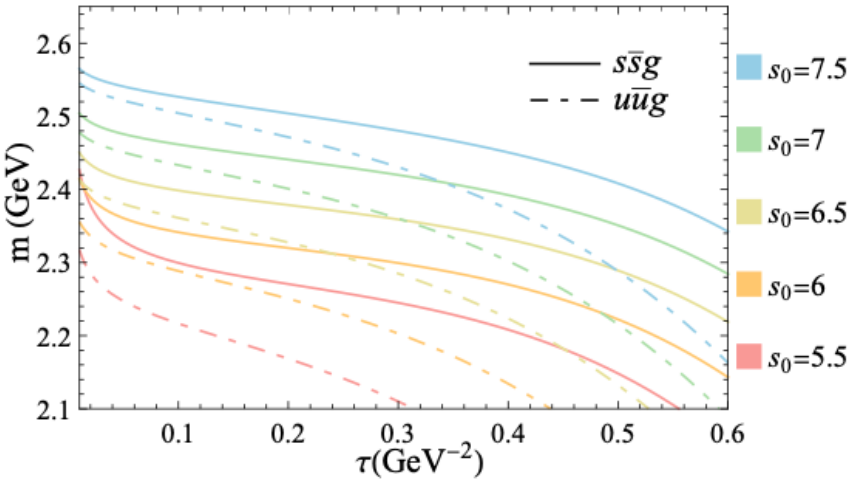

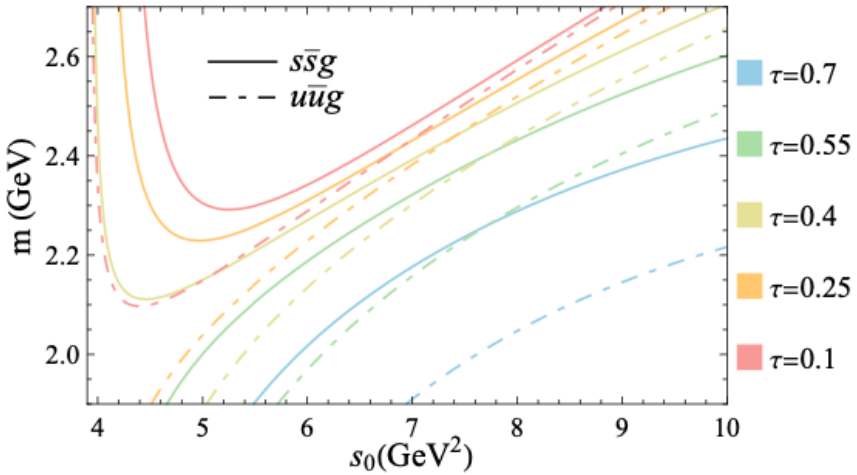

- **QSR at NLO:** $\mathbf{m_X \sim (2.2 - 2.4\ GeV)}$, which is much lower than the predicted result at the LO calculation!
- **LQCD:** $\mathbf{m_X \sim (2.2 - 2.5\ GeV)}$ PRD84(2011)074023;CPC45(2021)013112
- **Flux-tube model:** $\mathbf{m_X \sim (1.8 - 2.2\ GeV)}$ PRD52(1995)5242

NLO GSR analyses

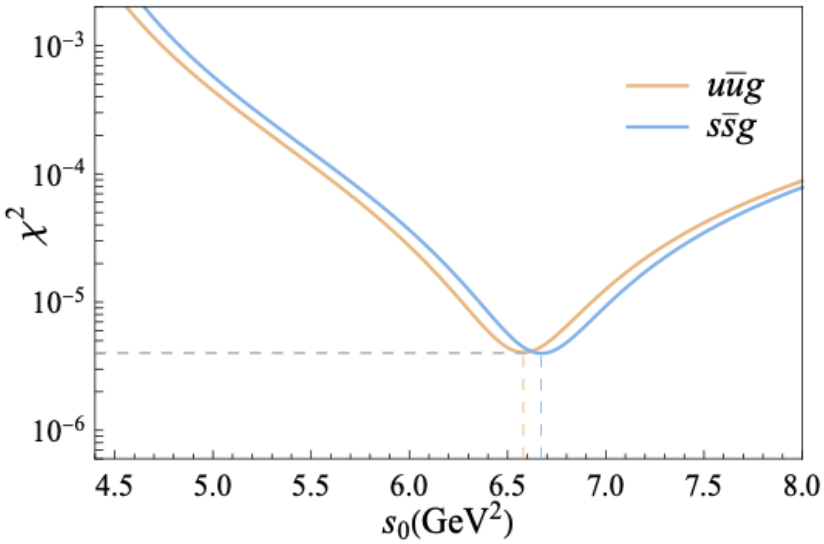

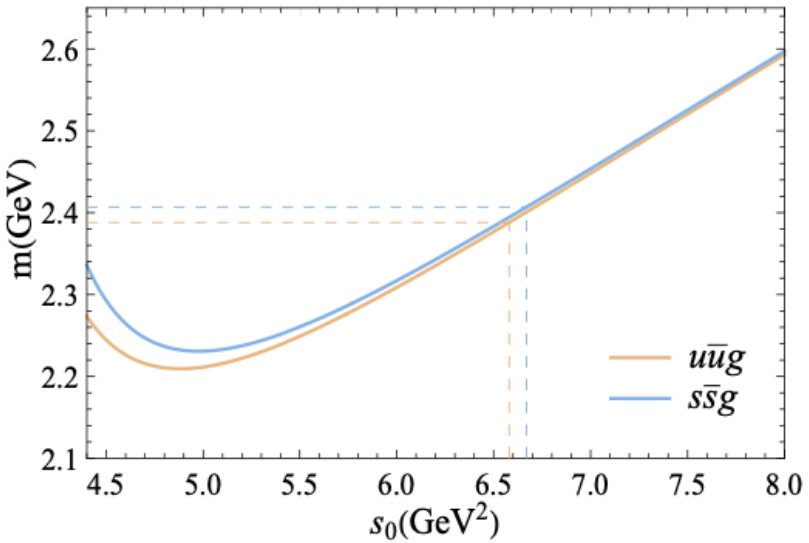

	NLO		NLO, excluding $d=8$ condensate		LO	
	$s\bar{s}g$	$u\bar{u}g$	$s\bar{s}g$	$u\bar{u}g$	$s\bar{s}g$	$u\bar{u}g$
$\overline{\chi^2_{\min}}$	2.63×10^{-6}	3.09×10^{-5}	4.23×10^{-6}	4.28×10^{-6}	2.24×10^{-5}	1.15×10^{-5}
$s_0(\mathrm{GeV}^2)$	5.87 ± 0.68	5.63 ± 1.04	6.67 ± 0.51	6.58 ± 0.50	9.08 ± 0.69	8.45 ± 0.74
$m(\mathrm{GeV})$	2.28 ± 0.12	2.22 ± 0.18	2.40 ± 0.09	2.39 ± 0.09	2.81 ± 0.10	2.72 ± 0.11

The predicted hybrid meson masses in both LSR and GSR are in consistent with the mass of $\phi(2170)$!

Summary

- The $\phi(2170)$ state was observed almost 20 years ago, but its nature is still unknown to date.
- The mass prediction at LO for the vector strangeonium hybrid meson is much higher than the mass of $\phi(2170)$.
- The NLO contributions are crucial for both perturbative term and nonperturbative condensates.
- The mass prediction at NLO is much lower than that at LO, supporting the hybrid meson interpretation of $\phi(2170)$!

Thank you very much!

Backup

Method II: Gaussian sum rules analyses (GSRs)

- The unsubtracted GSRs of integer weight k are defined as

$$G_k(\hat{s},\,\tau) = \sqrt{\frac{\tau}{\pi}} \lim_{\substack{N,\Delta^2\to\infty \\ \tau=\Delta^2/(4N)}} \frac{\left(-\Delta^2\right)^N}{\Gamma(N)} \times \left(\frac{d}{d\Delta^2}\right)^N \left\{ \frac{(\hat{s}+i\Delta)^k \Pi(-\hat{s}-i\Delta) - (\hat{s}-i\Delta)^k \Pi(-\hat{s}+i\Delta)}{i\Delta} \right\}$$
$$= \frac{1}{\sqrt{4\pi\tau}} \int_0^\infty t^k e^{-\frac{(\hat{s}-t)^2}{4\tau}} \frac{1}{\pi} \mathrm{Im}\Pi^{\mathrm{QCD}}(t)\,\mathrm{d}t\,,$$

  providing a fundamentally different weighting of the spectral function that makes them well-suited to analyzing distributed resonance strength hadron models.

- QCD Gaussian sum-rules:

$$G^{\mathrm{QCD}}(\hat{s},\,\tau,\,s_0) \equiv \frac{1}{\sqrt{4\pi\tau}} \int_0^{s_0} e^{-\frac{(\hat{s}-t)^2}{4\tau}} \frac{1}{\pi} \mathrm{Im}\Pi^{\mathrm{QCD}}(t) dt\,,$$

  where the GSRs have a duality interval of width $\sim\sqrt{2\tau}$ near $\hat{s}$. By varying the free parameter $\hat{s}$, GSRs can probe a wide region of the hadronic spectral function with the same sensitivity as the ground state region.

Gaussian sum rules analyses

The normalized GSRs (NGSRs) are defined as:

$$N^{\mathrm{QCD}}(\hat{s},\,\tau,\,s_0)=\frac{\frac{1}{\sqrt{4\pi\tau}}\int_0^{s_0}e^{-\frac{(\hat{s}-t)^2}{4\tau}}\rho^{\mathrm{had}}(t)\,\mathrm{d}t}{\int_0^{s_0}\rho^{\mathrm{had}}(t)\,\mathrm{d}t}.$$

In a double-narrow resonance model

$$\rho^{\mathrm{had}}(t)=f_1^2\delta\left(t-m_1^2\right)+f_2^2\delta\left(t-m_2^2\right)\,.$$

The normalized GSRs

$$N^{\mathrm{had}}\left(\hat{s},\,\tau\right)=\frac{1}{\sqrt{4\pi\tau}}\left(re^{-\frac{(\hat{s}-m_1^2)^2}{4\tau}}+(1-r)e^{-\frac{(\hat{s}-m_2^2)^2}{4\tau}}\right),$$

where the normalized couplings are defined as

$$r=\frac{f_1^2}{f_1^2+f_2^2}\,,1-r=\frac{f_2^2}{f_1^2+f_2^2}\,,0\leq r\leq 1.$$

Gaussian sum-rules analyses

Fitting the $\hat{s}$ dependence of the QCD prediction and hadronic model

$$\chi^2(r, m_2, s_0) = \sum_{\hat{s}_{min}}^{\hat{s}_{max}} \left[N^{\text{had}}(\hat{s}, \tau) - N^{\text{QCD}}(\hat{s}, \tau\, s_0) \right]^2 ,$$

with the modelled resonance $m_1 = m_{Y(2175)} = 2.188$ GeV.

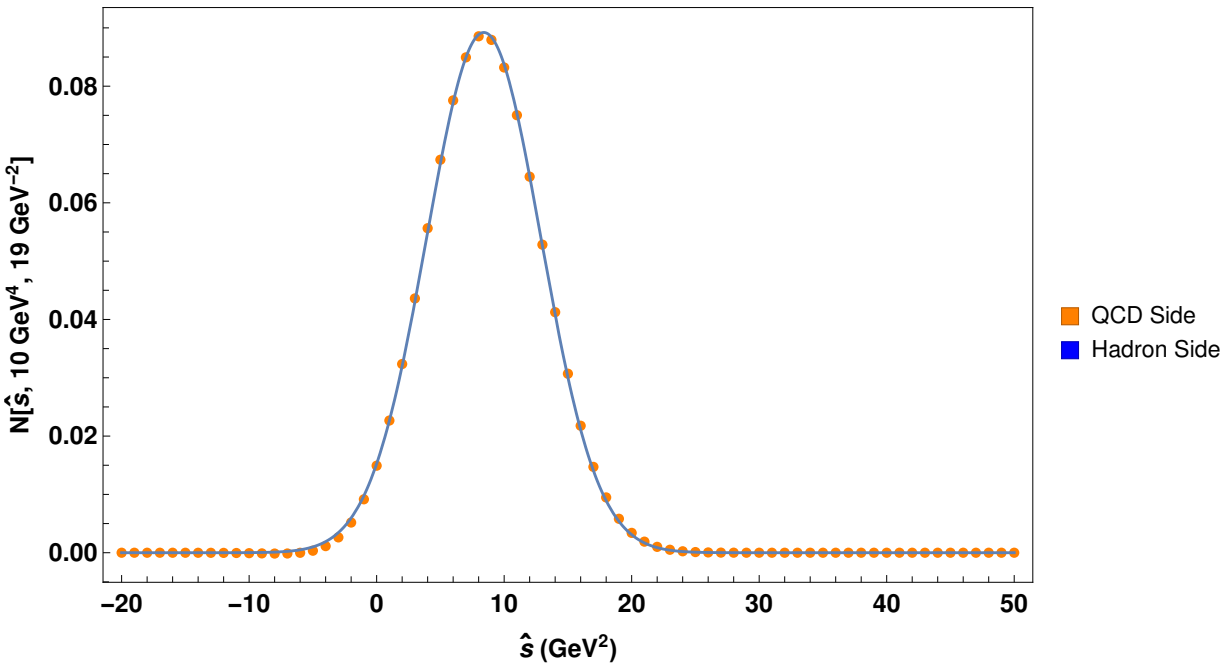

Gaussian sum-rules analyses

The resulting predictions:

$$s_0^{\rm opt} = 9.7 \pm 1.0\,{\rm GeV}^2$$
$$m_2 = m_{\rm fit} = 2.90 \pm 0.16\,{\rm GeV}$$
$$r \leq 0.033\,.$$

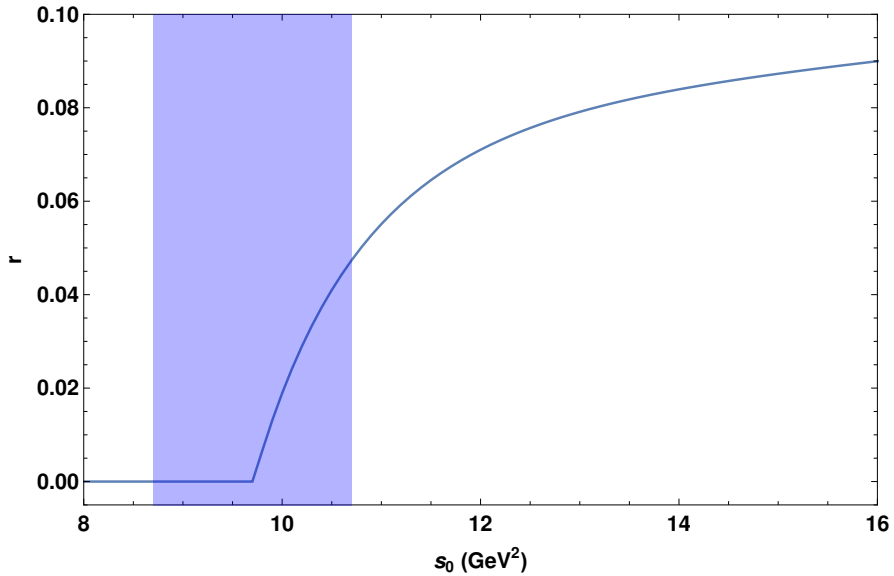

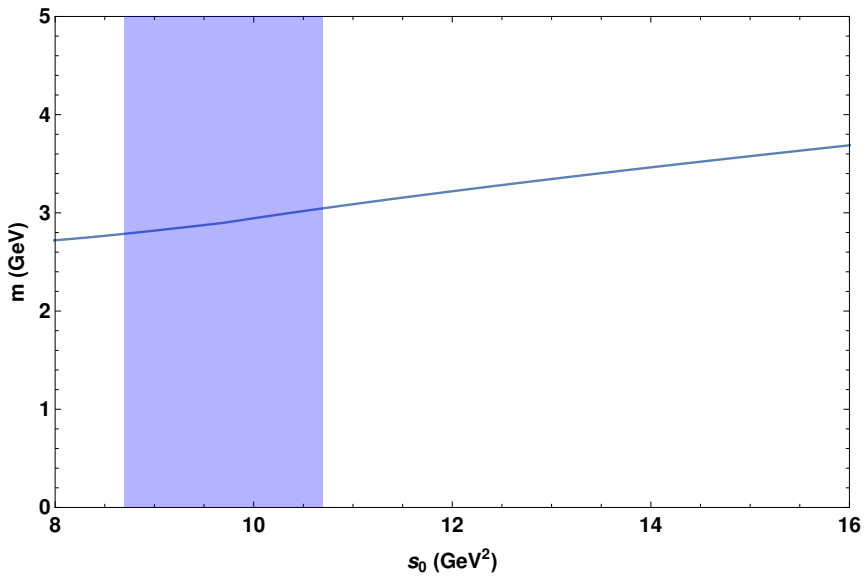

No evidence for a significant hybrid component of the $\phi(2170)$.